Research Article | Vol. 27, No. 3 | 4 Feb 2019 | OPTICS EXPRESS 2327
Optics EXPRESS

Quantum-limited fiber-optic phase tracking beyond π range

LIDAN ZHANG,[1] KAIMIN ZHENG,[1] FANG LIU,[1,2] WEI ZHAO,[3] LEI TANG,[1] HIDEHIRO YONEZAWA,[4] LIJIAN ZHANG,[1] YONG ZHANG,[1,*] AND MIN XIAO[1,5]

[1]*National Laboratory of Solid State Microstructures and College of Engineering and Applied Sciences, Nanjing University, Nanjing 210093, China*
[2]*Department of Physics, Nanjing Tech University, Nanjing 211816, China*
[3]*Department of Physics, Tsinghua University, Beijing 100084, China*
[4]*Centre for Quantum Computation and Communication Technology, School of Engineering and Information Technology, University of New South Wales, Canberra, Australian Capital Territory 2600, Australia*
[5]*Department of Physics, University of Arkansas, Fayetteville, AR 72701, USA*
[*]*zhangyong@nju.edu.cn*

Abstract: We experimentally demonstrate a fiber-based phase tracking system through an adaptive homodyne detection technique. In the experiment, we use a random phase signal as an example. The system works well when the random phase varies between −2.4 and + 2.4 radians. Such tracking range is much larger than previous work due to the improved performance of phase-locked loop. The minimum mean square error reaches theoretical value at a photon flux of ~10^6, which proves a quantum-limited fiber phase tracking. Such system has potential applications in high-precision real-time fiber sensing of temperature, strain, and so on.

1. Introduction

Optical phase tracking is a crucial task in precision metrology like gravitational-wave detection and biological measurements [1–9]. In a classical system, various sources of contamination such as impure probe states, imperfect detection, and poor data processing would limit the sensitivity of optical metrology [4,10]. To solve these problems, many techniques have been developed rapidly to suppress system noises, which allow measurements to reach quantum noise limit [9,11–13]. For example, heterodyne detection, one of the conventional way to estimate optical phase, can achieve a measurement accuracy that is only a factor of 2 greater than intrinsic uncertainty limit [14,15]. An alternative method using traditional homodyne detection can approach quantum noise limit. To measure a time-varying signal with a large phase range, adaptive homodyne detection with quantum-limited accuracy is developed in several precision measurement systems [16]. In 2012, a quantum-enhanced optical-phase tracking technique was reported [17], which has been studied extensively in other systems like mirror-motion estimation [18] and paradigmatic atomic sensors [19].

Previous experiments mainly focus on free-space optical measurements. With the rapid progresses in micro/nanotechnology, system miniaturization has become one of the current demands in phase sensors [20–22]. Many practical systems for measuring strain, temperature and other parameters are based on fibers as they have unparalleled advantages such as immunity to electromagnetic disturbance, flexible multiplexing and long-distance sensing [23,24]. For example, when monitoring real-time underwater signal, fiber is more reliable in comparison to the other systems [25,26]. To date, little efforts have tried to combine quantum-limited optical phase tracking technique with a fiber sensing system [2,27,28]. It is still difficult to reach quantum-limited sensitivity in most of fiber sensors [28]. The main

#348358 https://doi.org/10.1364/OE.27.002327
Journal © 2019 Received 16 Oct 2018; revised 15 Dec 2018; accepted 18 Dec 2018; published 25 Jan 2019

Optics EXPRESS

challenge in fiber is the large phase variations induced by the parameters to be measured. The low-frequency noise is also a tricky problem in a fiber system. In this letter, we construct a fiber homodyne system to detect a low-frequency random phase signal. To obtain optimal tracking, we design a phase-locked loop in the fiber homodyne system (i.e., adaptive fiber homodyne detection) and use a Kalman filter to estimate the time-varying phase precisely [29]. Our experimental results demonstrate a quantum-limited fiber homodyne system capable of tracking a random phase beyond the π range.

2. Theory

Consider an ideal adaptive balanced homodyne setup (Fig. 1). In our experiment, we use the double sideband mode as signal beam, which is generated by an electro-optic amplitude modulator (EOM). The double sideband mode is a balanced combination of upper and lower sidebands relative to the carrier frequency, which is equivalent to a weak coherent state [13]. In a general homodyne theory, the signal beam a and the strong local oscillator (LO) field L can be denoted as

$$a = [\alpha(e^{i(\omega+\Omega)t} + e^{i(\omega-\Omega)t}) + \delta\alpha]e^{i\Phi(t)} \tag{1}$$

$$L = (le^{i\omega t} + \delta l)e^{i\Phi_{LO}(t)} \tag{2}$$

Where ω denotes the optical carrier frequency, Ω the frequency of the amplitude modulation, $\Phi(t)$ the phase to be estimated, α and l are the amplitude operators of the signal and LO beams, and $\delta\alpha$ and δl are the fluctuation operators of the signal and LO beams with $\langle\delta\alpha\rangle = 0$ and $\langle\delta l\rangle = 0$, respectively. In homodyne detection, $l >> \alpha$, $l >> \delta l$, and $\alpha >> \delta\alpha$. The signal and LO beams are then combined in a beam splitter and detected by a pair of photodiodes. The phase-locked loop in Fig. 1 adjusts adaptively to ensure the relative phase of $\pi/2$ between the signal and LO beams, which is the operating point for homodyne detection [17]. After demodulation, the normalized homodyne output current can be written as [30]

$$I(t) = 2|\alpha|\sin\left[\Phi(t) - \Phi_f'(t)\right] + dW(t)/dt \tag{3}$$

where $\Phi_f'(t) = \Phi_{LO}(t) - \frac{\pi}{2}$ is the filtered estimate of $\Phi(t)$ and $dW(t)$ represents the quantum noise of the output current. For a coherent state, the quantum noise can be modeled as independent white Gaussian noise [10,31], satisfying $\langle dW(t)dW(\tau)\rangle = \delta(t-\tau)(dt)^2$. When the phase-locked loop well functions, $\Phi_f'(t)$ should be the real-time optimal estimate of $\Phi(t)$, which satisfies

$$\langle\left[\Phi(t) - \Phi_f'(t)\right]^2\rangle << 1 \tag{4}$$

Hence, Eq. (3) can be linearized as

$$I(t) \approx 2|\alpha|\left(\Phi(t) - \Phi_f'(t)\right) + dW(t)/dt \tag{5}$$

Optics EXPRESS

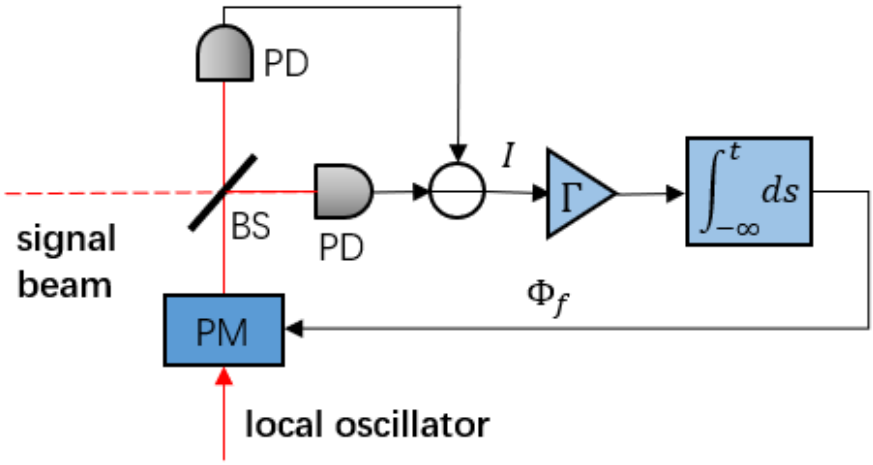

Fig. 1. Diagram of a homodyne phase-locked loop that implements the Kalman filtering estimation. The signal beam is combined with the local oscillator at a 50/50 beam splitter (BS) and then are detected by two photodetectors (PD). The outputs from the photodetectors are subtracted. The obtained current I is processed by a integrator($\int_{-\infty}^{t} ds$) with a Kalman gain (Γ), which determines an optimal phase estimate. The phase modulator (PM) is adjusted accordingly for the next estimate.

Considering the random signal as an Ornstein–Uhlenbeck (OU) process, the stochastic waveform Φ(t) can be defined by

$$d\Phi(t) = -\lambda\Phi(t)dt + \sqrt{\kappa}dV(t) \tag{6}$$

where dV(t) denotes the classical Wiener increment satisfying $\langle dV(t)dV(t_0)\rangle = \delta(t- t_0)(dt)^2$, λ the bandwidth of phase noise Φ(t), and κ/2λ the mean square variation of Φ(t).

During the tracking process, the homodyne output current I(t) is sampled at discrete times. Based on the Kalman-Bucy filtering theory, one can construct the real-time minimum mean square error (MSE) estimate of Φ(t) at the moment t, taking into account of the past measurement outcome {I(s): 0≤s≤t}. We define the estimator $\Phi'(t)$ as [29,32],

$$d\Phi'(t) = -\lambda\Phi'(t)dt + \Gamma I(t)dt \tag{7}$$

where Kalman gain is defined by $\Gamma = 4|\alpha|^2\Sigma(t)$ with $\Sigma(t) = \langle[\Phi(t)-\Phi_f'(t)]\otimes[\Phi(t)-\Phi_f'(t)]\rangle$. Σ(t) is the so-called covariance matrix of estimation that obeys

$$d\Sigma(t) = 2\lambda\Sigma(t)dt - 4|\alpha|^2(\Sigma(t))^2 dt + \kappa dt \tag{8}$$

At the steady state, Eq. (8) can be solved analytically to obtain minimum Σ(t) [29], which gives the optimal Kalman gain $\Gamma_{opt} = -\lambda + \sqrt{\lambda^2 + 4\kappa|\alpha|^2}$. Then, one can get the optimal estimate from Eq. (7) [17,29],

$$\Phi_f'(t) = \Gamma^{opt}\int_{-\infty}^{t} e^{-\lambda(t-s)}\frac{I(s)}{2|\alpha|}ds \tag{9}$$

Optics EXPRESS

It should be noted that according to the estimate $\Phi_f^{'}(t)$, the phase of LO beam is adjusted adaptively at the working point using the feedback loop illustrated in Fig. 1. Such adaptive system is capable to track a phase signal varying in a large range.

3. Experimental configuration and results

In our experiment, the input source is an ultra-narrow-linewidth 1064 nm Nd:YAG laser (Mephisto MOPA, Coherent Co.). The laser noise is suppressed to quantum noise limit through a "noise eater" feedback loop with a bandwidth of 2MHz. After coupled into a polarization-maintaining fiber, the laser is split to two beams at a fiber beam splitter (BS1). One beam is amplitude-modulated at 1.5 MHz using EOM1 to yield two sidebands, which can well avoid the low-frequency technical noises. The random phase signal Φ(t) is introduced through a piezoelectric transducer (PZT1). Here, we use a signal generator and a 1st-order low-pass filter with a cutoff frequency of 1 kHz to produce an OU random signal, which is amplified by a high voltage amplifier to drive PZT1. Correspondingly, the bandwidth of the fiber phase tracking system is set to be 1 kHz. The signal and LO beams interfere in another fiber beam splitter (BS2). The interference beams are then injected into a pair of balanced photodetectors and the two output photocurrents are subtracted to suppress the classical noises [10]. After demodulated by a lock-in amplifier, the homodyne output current I(t) is obtained.

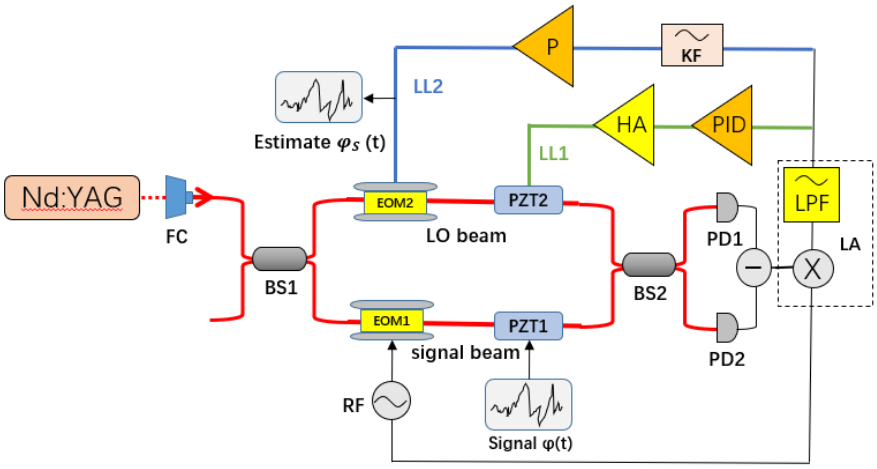

Fig. 2. Experimental configuration for adaptive homodyne measurements. The red and black lines denote optical and electrical paths, respectively. The green and blue lines denote the locking loop 1 (LL1) and locking loop 2 (LL2), respectively. FC: fiber coupler; BS: beam splitter; EOM: electro-optical modulator; PZT: piezoelectric transducer; PD: photodiode; RF: rf synthesizer; LPF: low pass filter; KF: Kalman filter; PID: PID servo; P: Proportion controller; HA: high-voltage amplifier; LA: Lock-in amplifier.

There are two phase-locked loops in Fig. 2, which lock the relative phase between the LO and signal beams at π/2. The first one (LL1) works at low frequencies (<100Hz) through PZT2, which can significantly suppress the environmental disturbances. The second loop (LL2) is used to implement the Kalman filtering estimation. In the experiment, we use a feedback low-pass filter with a cutoff frequency of 1 kHz after the demodulation current. The Kalman gain in this loop is adjusted by the proportion controller and a lock-in amplifier. The estimation term is generated and then fed back to the LO beam with EOM2. The data are stored as an estimated phase $\Phi^{'}(t)$ for the next analysis. We use a signal oscilloscope with a sampling rate of 350 MHz (MSO-X 3034T, KEYSIGHT) to record the waveform.

Optics EXPRESS

In our experiment, all the optical components in the adaptive homodyne system (Fig. 2) are polarization-maintaining fiber devices. The quantum efficiencies of the homodyne detectors are ~85%. With a 2.5 mW LO beam power, they produce 6.5 dB of shot noise on top of the electronic noise. The optical transmission efficiency of signal beam is 92% and the homodyne visibility is 97%. The resonance frequencies of PZT1 and PZT2 are about 30 kHz, which have a flat frequency response within the signal frequency domain (100Hz-1kHz) in our experiment.

Figure 3 gives the time-domain results of phase tracking. During the tracking process, the homodyne output current is kept near the zero point, which indicates that the relative phase between the signal beam and LO is well kept at the working point of $\pi/2$. The tracking system works well when the random phase varies between –2.4 and + 2.4 radians. The tracking range of phase rotation goes beyond π range, which indicates a promising fiber system for practical applications. In the experiment, the amplitude $|\alpha|^2$ of the coherent beam, the amplitude factor κ of the phase variance, and phase noise bandwidth λ are 1.43×10^6 s^{-1}, 7.91×10^3 rad/s, and 5.65×10^3 rad/s, respectively. It should be noted that the photon flux includes only the sideband modes considering that the carrier is removed after demodulation. The time constant of demodulation process is 1μs.

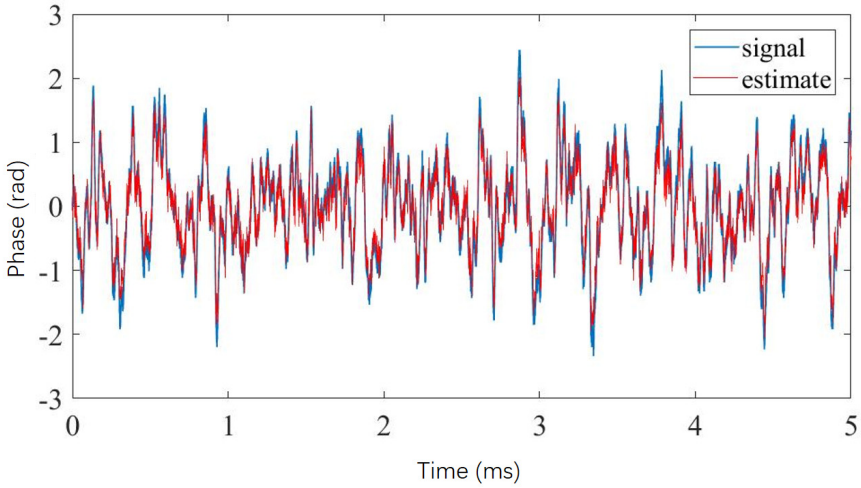

Fig. 3. Time domain results of fiber-based phase tracking. The blue curve is the input OU random signal with a bandwidth of 1 kHz and the red curve is the estimation result in our fiber homodyne system.

To analyze the phase-tracking performance quantitatively, we calculate the theoretical MSE using adaptive homodyne filter theory [17,29] to be

$$\sigma_{adap}^2 = \left\langle \left[\Phi(t) - \Phi_f^{'}(t) \right]^2 \right\rangle = \frac{-\lambda + \sqrt{\lambda^2 + 4\kappa|\alpha|^2}}{4|\alpha|^2} \tag{10}$$

For comparison, we also calculate the theoretical limit of a standard heterodyne system [11,15], which is

$$\sigma_{\text{hetero}}^2 = \left\langle \left[\Phi(t) - \Phi_{est}^{'}(t) \right]^2 \right\rangle = \frac{-\lambda + \sqrt{\lambda^2 + 4\kappa|\alpha|^2}}{2\sqrt{2}|\alpha|^2} \tag{11}$$

Optics EXPRESS

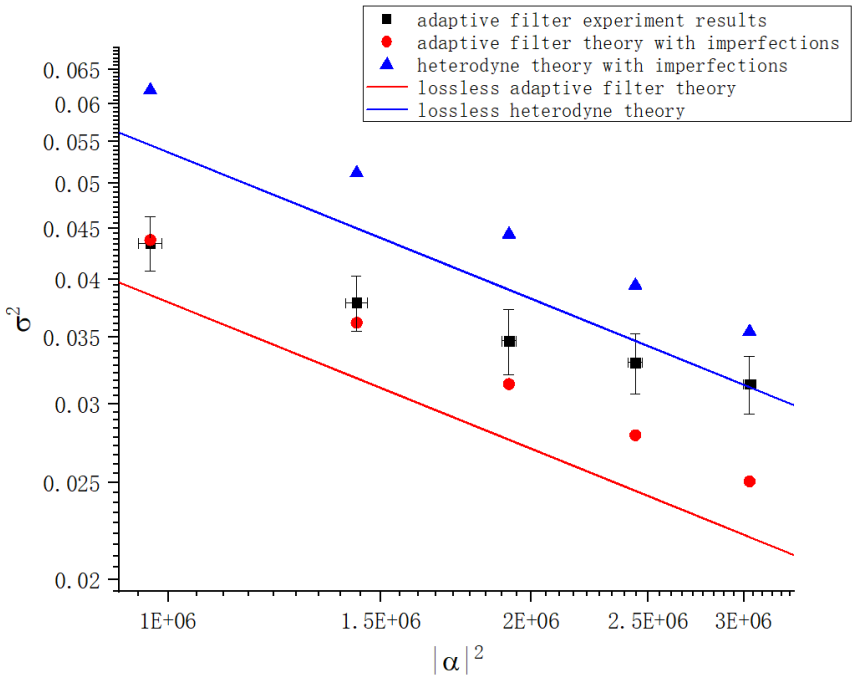

Fig. 4. Dependence of MSE σ^2 on $|\alpha|^2$. The black spots are the measured MSE. The red and blue spots are the simulated MSEs based on adaptive homodyne and heterodyne theories, respectively. In the calibration of the amplitude $|\alpha|^2$ for coherent beam, we has considered the imperfect efficiency of the system. The spots for adaptive homodyne and heterodyne theories are calculated including the experimental imperfections. If considering an ideal system without losses, the theoretical MSE can be further reduced as shown by the red and blue lines.

In the experiment, we adjust the modulation depth of EOM1 to change the photon flux $|\alpha|^2$ and calculate the corresponding MSEs. The values of κ and λ are the same as used in Fig. 3. When changing the photon flux, we adjust the Kalman gain to obtain the optimal tracking results. The experimental MSE is calculated from the data points with a signal of 5 ms. The standard deviation of MSE is obtained through 50 measurements. Figure 4 compares the experimental and theoretical MSEs for the tracking process of a random phase signal. Clearly, our experimental result goes beyond the theoretical value of a standard heterodyne system. At a photon flux of ~10^6, the measured MSE reaches theoretical value of the adaptive homodyne detection, which proves a quantum-limited random phase tracking in our fiber system. The discrepancy between the adaptive homodyne theory and experiment at a larger photon flux may stem from the technical noises in the phase-locked loop [14].

4. Conclusion

In this work, we have experimentally demonstrated a quantum-limited phase signal estimation using adaptive homodyne detection in fiber system. The random phase signal varying beyond the π range can be well tracked. Our system opens a door to achieve quantum-limited real-time detection in a fiber system, which can be utilized in various practical measurements such as high-precision remote sensing [22,24] and low-light biological measurement [2,3]. In addition, our system can be readily combined with a quantum light, which can perform quantum-enhanced phase tracking [17,18].

Optics EXPRESS

Funding

National Natural Science Foundation of China (NSFC) (91636106, 11874213, 11621091, 61605072), National Key R&D Program of China (2017YFA0303703, 2016YFA0302500), Fundamental Research Funds for the Central Universities (021314380105), and the Australian Research Council (ARC) Centre of Excellence for Quantum Computation and Communication Technology (CE170100012)

References

1. V. Giovannetti, S. Lloyd, and L. Maccone, "Advances in quantum metrology," Nat. Photonics **5**(4), 222–229 (2011).
2. N. P. Mauranyapin, L. S. Madsen, M. A. Taylor, M. Waleed, and W. P. Bowen, "Evanescent single-molecule biosensing with quantum-limited precision," Nat. Photonics **11**(8), 477–481 (2017).
3. M. A. Taylor, J. Janousek, V. Daria, J. Knittel, B. Hage, H.-A. Bachor, and W. P. Bowen, "Biological measurement beyond the quantum limit," Nat. Photonics **7**(3), 229–233 (2013).
4. C. M. Caves, "Quantum-mechanical noise in an interferometer," Phys. Rev. D Part. Fields **23**(8), 1693–1708 (1981).
5. M. Xiao, L. A. Wu, and H. J. Kimble, "Precision measurement beyond the shot-noise limit," Phys. Rev. Lett. **59**(3), 278–281 (1987).
6. C. Xia, D. Wang, Y. Wu, J. Guo, F. Liu, Y. Zhang, and M. Xiao, "Continuous-variable entanglement measurement using an unbalanced Mach-Zehnder interferometer," Opt. Lett. **40**(6), 1121–1124 (2015).
7. F. Liu, Y. Zhou, J. Yu, J. Guo, Y. Wu, S. Xiao, D. Wei, Y. Zhang, X. Jia, and M. Xiao, "Squeezing-enhanced fiber Mach-Zehnder interferometer for low-frequency phase measurement," Appl. Phys. Lett. **110**(2), 021106 (2017).
8. K. Goda, O. Miyakawa, E. E. Mikhailov, S. Saraf, R. Adhikari, K. McKenzie, R. Ward, S. Vass, A. J. Weinstein, and N. Mavalvala, "A quantum-enhanced prototype gravitational-wave detector," Nat. Phys. **4**(6), 472–476 (2008).
9. K. Jacobs, *Quantum measurement theory and its applications* (Cambridge University, 2014).
10. H.-A. Bachor and T. C. Ralph, *A guide to experiments in quantum optics* (Wiley, 2004).
11. D. W. Berry and H. M. Wiseman, "Adaptive quantum measurements of a continuously varying phase," Phys. Rev. A **65**(4), 043803 (2002).
12. M. Tsang, "Time-symmetric quantum theory of smoothing," Phys. Rev. Lett. **102**(25), 250403 (2009).
13. T. A. Wheatley, D. W. Berry, H. Yonezawa, D. Nakane, H. Arao, D. T. Pope, T. C. Ralph, H. M. Wiseman, A. Furusawa, and E. H. Huntington, "Adaptive optical phase estimation using time-symmetric quantum smoothing," Phys. Rev. Lett. **104**(9), 093601 (2010).
14. M. A. Armen, J. K. Au, J. K. Stockton, A. C. Doherty, and H. Mabuchi, "Adaptive homodyne measurement of optical phase," Phys. Rev. Lett. **89**(13), 133602 (2002).
15. D. Pope, H. Wiseman, and N. Langford, "Adaptive phase estimation is more accurate than nonadaptive phase estimation for continuous beams of light," Phys. Rev. A **70**(4), 043812 (2004).
16. J. Zhang, Y. Liu, R.-B. Wu, K. Jacobs, and F. Nori, "Quantum feedback: theory, experiments, and applications," Phys. Rep. **679**, 1–60 (2017).
17. H. Yonezawa, D. Nakane, T. A. Wheatley, K. Iwasawa, S. Takeda, H. Arao, K. Ohki, K. Tsumura, D. W. Berry, T. C. Ralph, H. M. Wiseman, E. H. Huntington, and A. Furusawa, "Quantum-enhanced optical-phase tracking," Science **337**(6101), 1514–1517 (2012).
18. K. Iwasawa, K. Makino, H. Yonezawa, M. Tsang, A. Davidovic, E. Huntington, and A. Furusawa, "Quantum-limited mirror-motion estimation," Phys. Rev. Lett. **111**(16), 163602 (2013).
19. R. Jiménez-Martínez, J. Kołodyński, C. Troullinou, V. G. Lucivero, J. Kong, and M. W. Mitchell, "Signal tracking beyond the time resolution of an atomic sensor by Kalman filtering," Phys. Rev. Lett. **120**(4), 040503 (2018).
20. J. L. Kou, M. Ding, J. Feng, Y. Q. Lu, F. Xu, and G. Brambilla, "Microfiber-based Bragg gratings for sensing applications: a review," Sensors (Basel) **12**(7), 8861–8876 (2012).
21. J. Lou, Y. Wang, and L. Tong, "Microfiber optical sensors: a review," Sensors (Basel) **14**(4), 5823–5844 (2014).
22. Y. Xu, P. Lu, L. Chen, and X. Bao, "Recent developments in micro-structured fiber optic sensors," Fibers (Basel) **5**(1), 3 (2017).
23. B. Lee, "Review of the present status of optical fiber sensors," Opt. Fiber Technol. **9**(2), 57–79 (2003).
24. L. Mescia and F. Prudenzano, "Advances on Optical Fiber Sensors," Fibers (Basel) **2**(1), 1–23 (2013).
25. G. A. Cranch, P. J. Nash, and C. K. Kirkendall, "Large-scale remotely interrogated arrays of fiber-optic interferometric sensors for underwater acoustic applications," IEEE Sens. J. **3**(1), 19–30 (2003).
26. J. E. Parsons, C. A. Cain, and J. B. Fowlkes, "Cost-effective assembly of a basic fiber-optic hydrophone for measurement of high-amplitude therapeutic ultrasound fields," J. Acoust. Soc. Am. **119**(3), 1432–1440 (2006).
27. H. M. Wiseman and G. J. Milburn, *Quantum measurement and control* (Cambridge University, 2009).
28. S. Stepanov, M. P. Sánchez, and E. H. Hernández, "Noise in adaptive interferometric fiber sensor based on population dynamic grating in erbium-doped fiber," Appl. Opt. **55**(26), 7324–7329 (2016).
29. M. Tsang, J. H. Shapiro, and S. Lloyd, "Quantum theory of optical temporal phase and instantaneous frequency.

Optics EXPRESS

II. Continuous-time limit and state-variable approach to phase-locked loop design," Phys. Rev. A **79**(5), 053843 (2009).
30. H. Wiseman and R. Killip, "Adaptive single-shot phase measurements: The full quantum theory," Phys. Rev. A **57**(3), 2169–2185 (1998).
31. C. Gardiner, P. Zoller, and P. Zoller, *Quantum noise: a handbook of Markovian and non-Markovian quantum stochastic methods with applications to quantum optics* (Springer Science & Business Media, 2004).
32. A. B. Baggeroer, *State variables and communication theory* (MIT, 1970).